Intracrystalline Deuteration of Native Cellulose

Yoshiharu Nishiyama,[†] Akira Isogai,[†] Takeshi Okano,[†] Martin Müller,[§] and Henri Chanzy*[,‡]

Graduate School of Agricultural and Life Science, The University of Tokyo, Yayoi, Tokyo 113-8256, Japan; European Synchrotron Radiation Facility, B.P. 220, 38043 Grenoble Cedex, France; and Centre de Recherches sur les Macromolecules Végétales, CNRS, affiliated with the Joseph Fourier University of Grenoble, BP 53, 38041 Grenoble Cedex 9, France

Received October 6, 1998
Revised Manuscript Received January 5, 1999

Introduction. It has been known for several decades that the accessible OH groups of cellulose could be reversibly converted to ODs when the samples were subjected to D_2O in either the vapor or liquid state.[1−4] This deuteration phenomenon, which is commonly monitored by Fourier transform infrared (FT-IR) spectroscopy, leads to one of the best techniques available today to measure the accessibility of cellulose.[5] The ease of the hydrogen−deuterium exchange in the accessible hydroxyl groups of cellulose has also been used for neutron scattering studies. In a classical experiment with cellulose II fortisan fibers, a meaningful fiber periodicity of 150−200 Å was revealed by small-angle neutron scattering after exposing the fibers to D_2O vapors.[6] The mercerization of cotton cellulose in NaOD has been another experiment that has led to the recording of deuterated neutron fiber diffraction diagrams that differed substantially from the corresponding hydrogenated patterns.[7] In such deuterated samples, all the hydroxyl groups, including the intracrystalline ones, were deuterated. The difference existing between the OH and OD neutron fiber diagrams have not been fully exploited so far. When the experiments and calculations will be complete, one expects to obtain the exact crystallographic position of the hydrogen engaged in the intracrystalline hydrogen-bonding network.

To our knowledge, there are two reports where the intracrystalline deuteration of native cellulose has been described.[8,9] In one of them, the authors used a number of cycles where cellulose was repeatedly dried and rewetted in D_2O at temperatures of up to 100 °C. This technique, which led to nearly total intracrystalline deuteration of wood cellulose after more than 100 cycles, was less effective for cellulose samples of higher crystallinity.[8] The second report[9] describes how purified *Halocynthia* samples could be deuterated when subjected to the hydrothermal technique of Yamamoto et al.,[10] but after replacing NaOH and H_2O by NaOD and D_2O, respectively. Typically, the samples treated at 260 °C for 30 min in the presence of 0.1 N NaOD showed time-of-flight neutron powder diffraction profiles that differed markedly from the corresponding hydrogenated sample.[9]

In the present work, the hydrothermal intracrystalline deuteration method[9] was investigated further, using either cellulose I_α- or I_β-rich samples of high crystallinity. The experiments that were achieved on oriented films of cellulose microcrystals were followed by electron microscopy, X-ray diffraction analysis, and FT-IR polarized spectroscopy.

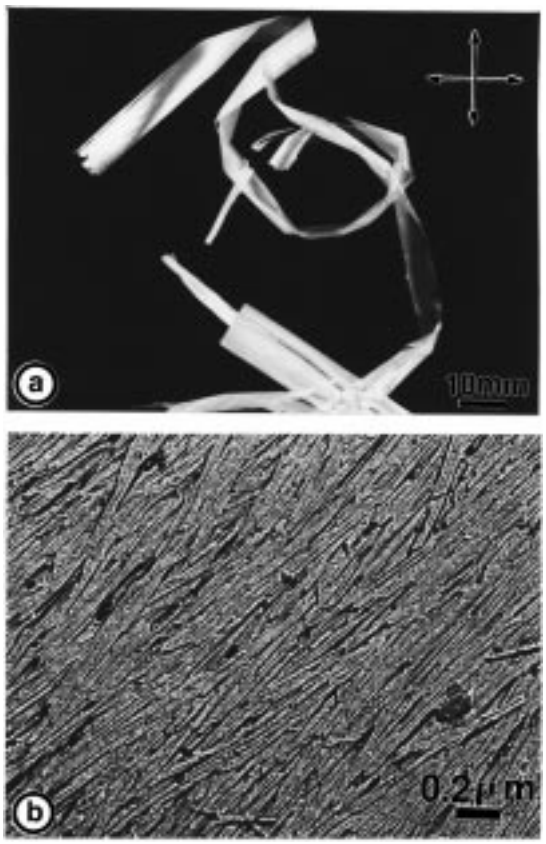

Figure 1. (a) Films made of oriented cellulose microcrystals of *Halocynthia* and visualized between crossed polaroids. The double-headed arrows indicate the direction of the axes of the polarizers. (b) Surface replica after shadow-casting with Pt/C of a film such as in (a).

Experimental Section. *Uniaxially Oriented Films of Cellulose***.** Two types of highly crystalline cellulose samples were used in this study, namely a sample of tunicate cellulose from *Halocynthia* that consisted almost of pure I_β cellulose and a sample of *Cladophora* that contained about 70% cellulose I_α.[11] The tunicate cellulose was extracted from the mantle of *Halocynthia roretzi*. It was deproteinized and bleached as described elsewhere.[12] This sample was then hydrolyzed overnight in 50% (w/w) aqueous sulfuric acid at 40 °C to yield a suspension of tunicate cellulose microcrystals. The sample from *Cladophora* cell wall was first decalcified by boiling into 1 N HCl for 1 h. It was then bleached and hydrolyzed into microcrystals, using the same hydrolyzing conditions as in the case of tunicate cellulose.

Films of oriented microcrystals of cellulose from tunicate and *Cladophora* were prepared following an earlier description.[13]

*Intracrystalline Deuteration of Cellulose***.** For both samples, the cellulose films were inserted in glass ampules filled with 0.1 N NaOD/D_2O. The ampules were sealed and positioned inside pressure vessels half full

* Author for correspondence.
† University of Tokyo.
§ European Synchrotron Radiation Facility.
‡ CNRS.

10.1021/ma981563m CCC: $18.00
Published on Web 02/26/1999

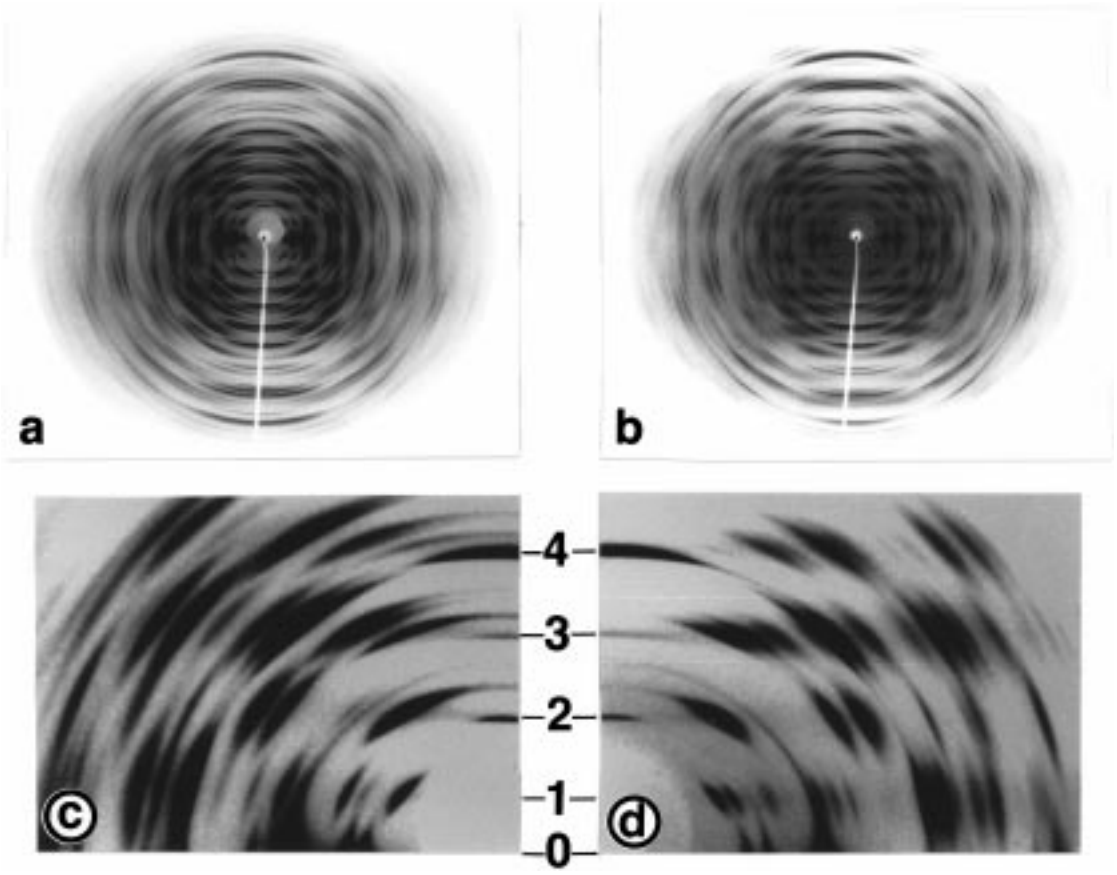

Figure 2. (a) Synchrotron X-ray fiber diagrams of deuterated *Halocynthia* (I_β cellulose) with fiber axis vertical. (b) Same as in (a), but with deuterated *Cladophora* ($I_\alpha + I_\beta$ cellulose). (c) and (d), which display the inner part of the diagrams, are respectively enlarged from (a) and (b). In (c) and (d) the equatorial as well as the first four layer lines are outlined.

with water to act as counter pressure. These vessels were heated to 210 °C, and this temperature was kept for 30 min. Such temperature was selected as being below the point of solid-state conversion of cellulose I_α into I_β but sufficiently high to exchange the intracrystalline OH moieties of cellulose by ODs.

Infrared Spectroscopy. Films of about 1 μm in thickness that displayed a strong birefringence were mounted on microdisks with an opening of 500 μm in diameter. These films were analyzed by FT-IR in the range 4000−400 cm^{-1} using a Perkin-Elmer 1720X spectrophotometer equipped with a microfocus accessory and a gold wire polarizer. All spectra were recorded with a resolution of 2 cm^{-1}. In these spectra, the transmission was at least of 15% at any wavelength. The spectra were recorded in the transmission mode and converted into absorption for display.

Electron Microscopy. Thick films of cellulose microcrystals were shadow-casted with platinum carbon at an angle of 30° followed by backing with carbon. The cellulose was then dissolved overnight in 70% (w/w) H_2SO_4, and the resulting replica were washed with distilled water, mounted on electron microscopy grids, and observed with a Philips CM200 CRYO operated at 80 kV.

X-ray Diffraction. The 0.2 mm thick samples were analyzed at the ID2 biocrystallography beamline at the European Synchrotron Radiation Facility (ESRF), Grenoble, France.[14] The samples, which were positioned at the center of a Huber five-circle goniometer, were irradiated for 20 s with X-rays (wavelength 0.720 006 Å). The diffraction data were recorded with a 345 mm MAR imaging plate scanner positioned at 170 mm from the sample.

Results and Discussion. Typical features of the oriented cellulose films used in this study are presented in Figure 1a,b. These images, shown here for *Halocynthia* cellulose samples, indicate that each film consisted of an arrangement of micron-sized cellulose microcrystals neatly packed with respect to one another and indicating a fairly good longitudinal orientation. This orientation as well as the crystallinity of the films was revealed by the X-ray fiber diagrams taken on hydrogenated and deuterated samples. For a given cellulose specimen, no specific difference could be detected between the hydrogenated and deuterated diagrams. Here, we show the deuterated patterns for *Halocynthia* (Figure 2a,c) and *Cladophora* (Figure 2b,d) specimens. Both diagrams, which are of the fiber type, confirm not only the integrity of the cellulose I character but also the high crystallinity of the samples as they display a resolution of the order of 1 Å. As expected, the diagram in Figure 2c presents a fairly intense meridional reflection at 5.2 Å on the second layer line. This reflection, which is one of the signatures of I_β cellulose,[15] is somewhat weaker in the pattern of *Cladophora* (Figure 2d). Other marked differences between the diagrams in parts c and d of Figure 2 are clearly observed in the first and third layer lines. In these lines, all the spots observed in Figure 2c are also seen in Figure 2d, but with different intensities. In addition, there are spots in Figure 2d that are not present in Figure 2c. Thus, the pattern in 2d can be considered as a subset of the pattern in Figure 2c as expected from the I_α/I_β composi-

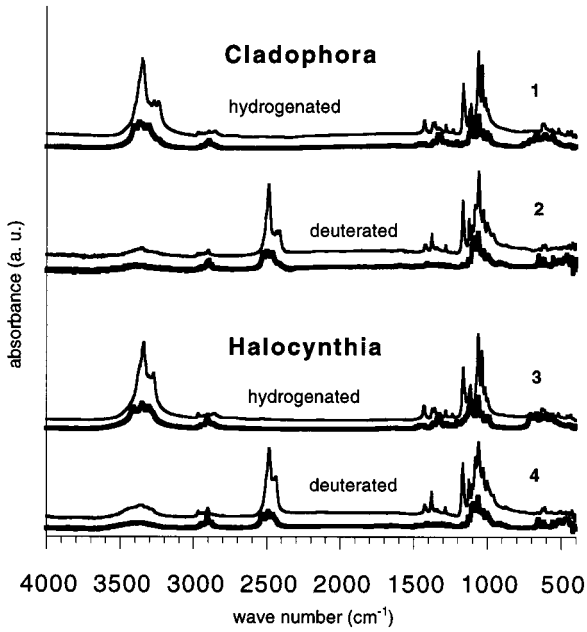

Figure 3. Series of polarized FT-IR spectra recorded on oriented films of *Halocynthia* and *Cladophora* cellulose microcrystals, before and after intracrystalline deuteration. The spectra in thin lines correspond to the parallel situation where the axis of the polarizer is aligned parallel with respect to the microcrystal axes. The spectra in bold line correspond to the perpendicular situation. Spectra 1 and 2 are from *Cladophora*, and spectra 3 and 4 are from *Halocynthia*.

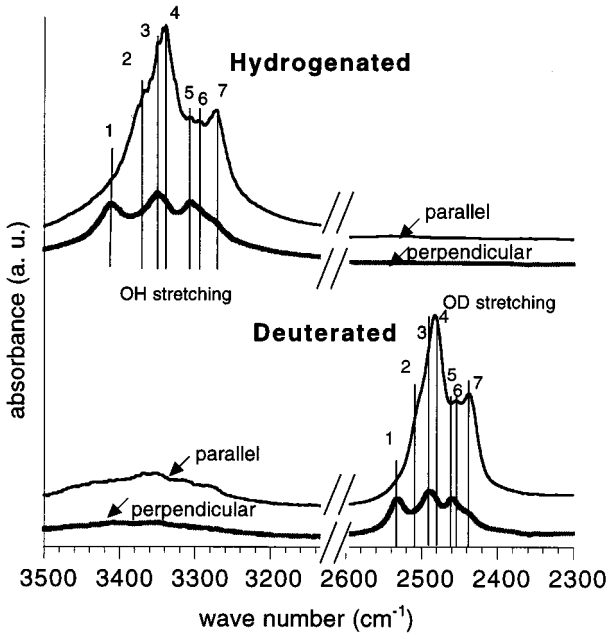

Figure 4. Enlargement from Figure 3 showing the OH and OD stretching regions of the polarized infrared spectra of *Halocynthia* microcrystals. In the hydrogenated spectra, lines 1−7 correspond respectively to absorption bands near 3411, 3370, 3351, 3339, 3305, 3294, and 3272 cm^{-1}. These bands are shifted in the deuterated spectra to near 2532, 2509, 2490, 2480, 2458, 2450, and 2437 cm^{-1}.

tion of *Cladophora* cellulose. This composition and the relative amount of I_α and I_β phases appear unaffected by the hydrothermal treatment leading to the deuteration of the samples.

In Figures 3−5 are shown some of the polarized FT-IR spectra that were recorded from the films of *Halocynthia* and *Cladophora* microcrystals before and after

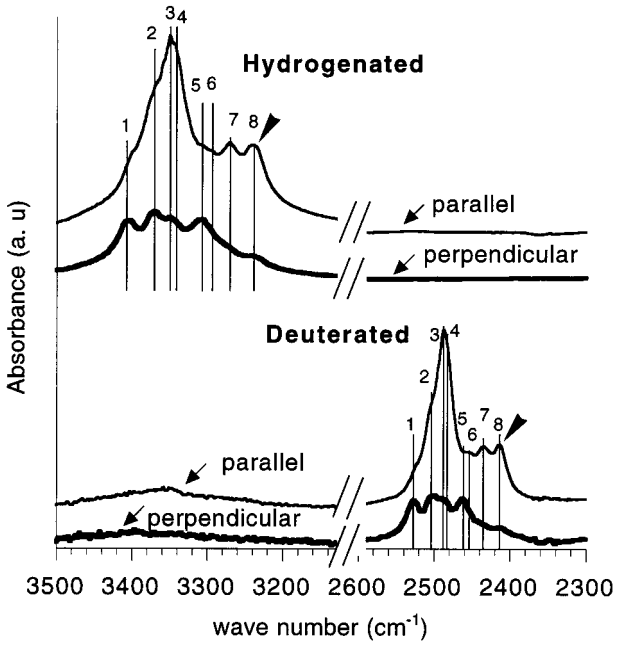

Figure 5. As in Figure 4, but for *Cladophora*. In the initial spectra, the bands labeled 1−8 correspond to absorption bands near 3405, 3371, 3350, 3342, 3307, 3293, 3271, and 3238 cm^{-1}. These bands are shifted in the deuterated spectra to near 2527, 2503, 2487, 2482, 2461, 2453, 2434, and 2414 cm^{-1}. The arrows point to the absorption bands that are specific of I_α cellulose.

intracrystalline deuteration. The spectra in Figure 3 correspond to the full width 4000−400 cm^{-1}. Their comparison presents a number of interesting features: (i) upon deuteration, the series of sharp OH stretching infrared bands located around 3500−3300 cm^{-1} became completely translated by about 1000 cm^{-1} toward lower wavelengths without loss of resolution; (ii) most of the bands corresponding to the CH stretching modes and located around 3000−2800 cm^{-1} appeared unaffected by the deuteration; (iii) in the region 1500−1000 cm^{-1} as well as in the region 700−400 cm^{-1}, a substantial amount of band shifting occurred.

In Figures 4 and 5 are shown some enlargements of the OH stretching region of both *Halocynthia* and *Cladophora* cellulose before and after deuteration. For both samples, the intracrystalline deuteration appeared quite perfect as all the sharp features of the OH stretching region were translated to the OD stretching region for both samples. In the case of initial *Cladophora*, the absorption band located at around 3240 cm^{-1} that is specific of cellulose I_α is shifted to around 2415 cm^{-1} without any loss of intensity. This is an indication that the applied hydrothermal annealing treatment was achieved at a temperature sufficiently low to avoid any $I_\alpha \rightarrow I_\beta$ conversion that is known to occur at a higher temperature.

The results obtained in this study present a number of interesting features that should be quite useful for improving the current knowledge of the structure and spectroscopy of cellulose in relation with its polymorphism. The recording of spectra such as shown in Figure 3 is not only interesting for the OH/OD stretching region. They should also be valuable to assign other parts of the infrared spectra, and this could be extended also to Raman spectra as well.

One of the best interests in preparing oriented crystalline films of hydrogenated and deuterated native cellulose is their use for the recording of high-resolution

neutron fiber diagrams with ODs and OHs. The difference in contrast between these diagrams could be used to calculate meaningful Fourier difference maps leading to the visualization of the H atoms of the hydroxyl groups. Thus, one should have access for the first time to a clear definition of the hydrogen bonds that hold the structure of cellulose together. Such a technique was applied recently with great success to the precise location of water molecules in fibers of DNA with the D and A conformations.[16] Substantial advances for the localization of hydration water were also obtained in the case of hyaluronic acid.[17] In preliminary experiments, deuterated as well as hydrogenated films such as the one shown here gave neutron fiber diagrams presenting the same resolution as the X-ray diffraction diagrams in Figure 2.[18] These neutron fiber diagrams, which present substantial difference between the H and the D samples, are presently being analyzed with the goal of refining the definition of the hydrogen bonds in cellulose I_α and I_β.

Acknowledgment. Y.N. thanks the French government and the Japan Society for the Promotion of Science for financial support. We thank also B. Rasmussen of EMBL, Grenoble, for his help with the synchrotron experiments.

References and Notes

(1) Frilette, V. J.; Hanle, J.; Mark, H. *J. Am. Chem. Soc.* **1948**, *70*, 1107−1113.
(2) Mann, J.; Marrinan, H. J. *Trans. Faraday Soc.* **1956**, *52*, 481−487.
(3) Mann, J. In *Methods in Carbohydrate Chemistry;* Whistler, R. L., Ed.; Academic Press: New York, 1963; Vol. III, pp 114−119.
(4) Jeffries, R. *Polymer* **1963**, *4*, 375−389.
(5) Rowland, S. P.; Bertonière, N. In *Cellulose Chemistry and its Applications*; Nevell, T. P., Zeronian, S. H., Eds.; Ellis Horwood Ltd.: Chichester, 1985; pp 112−137.
(6) Fischer, E. W.; Herchenröder, P.; St. J. Manley, R.; Stamm, M. *Macromolecules* **1978**, *11*, 213−217.
(7) Langan, P.; Denny, R. C.; Mahendrasingam, A.; Mason, S. A.; Jaber, A. *J. Appl. Crystallogr.* **1996**, *29*, 383−389.
(8) Sepall, O.; Mason, S. G. *Can. J. Chem.* **1961**, *39*, 1944−1955.
(9) Wada, M.; Okano, T.; Sugiyama, J. *Cellulose* **1997**, *4*, 221−232.
(10) Yamamoto, H.; Horii, F.; Odani, H. *Macromolecules* **1989**, *22*, 4130−4132.
(11) Imai, T.; Sugiyama, J. *Macromolecules* **1998**, *31*, 6275−6279.
(12) Favier, V.; Chanzy, H.; Cavaillé, J−Y. *Macromolecules* **1995**, *28*, 6365−6367.
(13) Nishiyama, Y.; Kuga, S.; Wada, M.; Okano, T. *Macromolecules* **1997**, *30*, 6395−6397.
(14) Bösecke, P.; Diat, O.; Rasmussen, B. *Rev. Sci. Instrum.* **1995**, *66*, 1636−1638.
(15) Sugiyama, J.; Chanzy, H.; Vuong, R. *Macromolecules* **1991**, *24*, 4168−4175.
(16) Fuller, W.; Forsyth, V. T.; Mahendrasingam, A.; Langan, P.; Pigram, W. J.; Mason, S. A.; Wilson, C. C. In *Neutron in Biology*; Schoenborn, B. P., Knott, R., Eds.; Plenum Press: New York, 1996; pp 345−358.
(17) Deriu, A.; Cavatorta, F.; de Micheli, T.; Rupprecht, A.; Langan, P. *Physica B* **1997**, *234−236*, 215−216.
(18) Nishiyama, Y.; Okano, T.; Langan, P.; Chanzy, H. *Int. J. Biol. Macromol.*, in press.

MA981563M